UNIVERSITY OF BIRMINGHAM
University of Birmingham Research at Birmingham

Intranasal exposure to ZnO nanoparticles induces alterations in cholinergic neurotransmission in rat brain

Guo, Zhiling; Zhang, Peng; Luo, Yali; Xie, Heidi Qunhui; Chakraborty, Swaroop; Monikh, Fazel Abdolahpur; Bu, Lijing; Liu, Yiyun; Ma, Yongchao; Zhang, Zhiyong; Valsami-Jones, Eugenia; Zhao, Bin; Lynch, Iseult

DOI:
10.1016/j.nantod.2020.100977

License:
Creative Commons: Attribution-NonCommercial-NoDerivs (CC BY-NC-ND)

Document Version
Publisher's PDF, also known as Version of record

Citation for published version (Harvard):
Guo, Z, Zhang, P, Luo, Y, Xie, HQ, Chakraborty, S, Monikh, FA, Bu, L, Liu, Y, Ma, Y, Zhang, Z, Valsami-Jones, E, Zhao, B & Lynch, I 2020, 'Intranasal exposure to ZnO nanoparticles induces alterations in cholinergic neurotransmission in rat brain', *Nano Today*, vol. 35, 100977. https://doi.org/10.1016/j.nantod.2020.100977

Link to publication on Research at Birmingham portal

General rights
Unless a licence is specified above, all rights (including copyright and moral rights) in this document are retained by the authors and/or the copyright holders. The express permission of the copyright holder must be obtained for any use of this material other than for purposes permitted by law.

•Users may freely distribute the URL that is used to identify this publication.
•Users may download and/or print one copy of the publication from the University of Birmingham research portal for the purpose of private study or non-commercial research.
•User may use extracts from the document in line with the concept of 'fair dealing' under the Copyright, Designs and Patents Act 1988 (?)
•Users may not further distribute the material nor use it for the purposes of commercial gain.

Where a licence is displayed above, please note the terms and conditions of the licence govern your use of this document.

When citing, please reference the published version.

Take down policy
While the University of Birmingham exercises care and attention in making items available there are rare occasions when an item has been uploaded in error or has been deemed to be commercially or otherwise sensitive.

If you believe that this is the case for this document, please contact UBIRA@lists.bham.ac.uk providing details and we will remove access to the work immediately and investigate.

Download date: 23. Apr. 2024

Nano Today 35 (2020) 100977

Contents lists available at ScienceDirect

Nano Today

journal homepage: www.elsevier.com/locate/nanotoday

Intranasal exposure to ZnO nanoparticles induces alterations in cholinergic neurotransmission in rat brain

Zhiling Guo[a,b,c], Peng Zhang[c,*], Yali Luo[a,b], Heidi Qunhui Xie[a,b,d], Swaroop Chakraborty[e], Fazel Abdolahpur Monikh[f], Lijing Bu[g], Yiyun Liu[a,b], Yongchao Ma[a,b], Zhiyong Zhang[h], Eugenia Valsami-Jones[c], Bin Zhao[a,b,d,**], Iseult Lynch[c]

[a] State Key Laboratory of Environmental Chemistry and Ecotoxicology, Research Center for Eco-Environmental Sciences, Chinese Academy of Sciences, Beijing 100085, China
[b] University of Chinese Academy of Sciences, Beijing 100049, China
[c] School of Geography, Earth and Environmental Sciences, University of Birmingham, Edgbaston, Birmingham B15 2TT, UK
[d] Institute of Environment and Health, Hangzhou Institute for Advanced Study, University of Chinese Academy of Sciences, Hangzhou 310024, China
[e] Department of Biological Engineering, Indian Institute of Technology, Gandhinagar, Gujarat, 382355, India
[f] Institute of Environmental Sciences (CML), Leiden University, Leiden 2300 RA, the Netherlands
[g] Center for Evolutionary and Theoretical Immunology (CETI), Department of Biology, University of New Mexico, Albuquerque, NM, 87131, USA
[h] Institute of High Energy Physics, Chinese Academy of Sciences, Beijing 100049, China

ARTICLE INFO

Article history:
Received 3 May 2020
Received in revised form 30 August 2020
Accepted 31 August 2020
Available online 17 September 2020

Keywords:
Zinc oxide nanoparticles
Brain
Cholinergic neurotransmission
Acetylcholine
Acetylcholinesterase

ABSTRACT

The neurotoxicity of inhaled ZnO nanoparticles (NPs) and the underlying mechanisms remain largely unknown. In this study, ZnO NPs (30 ± 6 nm) were intranasally instilled to rats *via* a single dose (13 mg Zn/kg BW), with $ZnSO_4$ as the ionic control, and analysis 7-days post exposure. The hippocampus was found to be the main target for Zn accumulation for both ZnO NPs and $ZnSO_4$. Synchrotron radiation based X-ray absorption fine structure (XAFS) analysis showed that no particulate ZnO was found, suggesting the occurrence of dissolution and transformation of ZnO NPs. Multi-omics analysis, including transcriptomics, proteomics and metabolomics, demonstrated that cholinergic neurotransmission was the main biological process affected following both treatments. The release of the key neurotransmitter acetylcholine (ACh) was increased by enhanced ACh synthesis, upregulation of vesicular ACh transporter, and suppression of the activity of ACh hydrolysis enzyme (AChE), either by direct Zn-AChE interaction or a transcriptional down-regulation mechanism. In addition, ZnO NPs and $ZnSO_4$ induced similar molecular consequences and exhibited the same Zn chemical speciation (100 % of Zn complexes) in the hippocampal region evidenced by XAFS analysis, suggesting that the observed biological effects were mainly derived from Zn^{2+} released from the ZnO NPs. This study not only evidences a new pathway for the impact of ZnO NPs on the brain, but also identifies the origin of the impact as ionic Zn, which provides the basis for safe-by-design of ZnO NPs.

© 2020 The Author(s). Published by Elsevier Ltd. This is an open access article under the CC BY-NC-ND license (http://creativecommons.org/licenses/by-nc-nd/4.0/).

Introduction

The advent of nanotechnology has sparked a wave of novel commercial products from machines to medicines, bringing profound social and economic benefits. In parallel, the potential human health risks due to the unprecedented avenues of human exposure to nanoparticles (NPs) are increasingly a cause for concern [1]. Comprehensive understanding of the toxicity of NPs can lead to safer design and reduce the side effects or unintended consequences of NPs.

ZnO NPs are among the three most produced nanomaterials (the other two being TiO_2 NPs and SiO_2 NPs) with a global production of more than 550 tons per year [2]. They have been utilized in various applications due to their unique photocatalytic, electronic, optical, dermatological, and antibacterial properties. Their most common applications are in beauty care products, sunscreens, food additives, cements, and fabric treatments for UV blocking [3–5]. Moreover, their potential applications in the biomedical field have received

* Corresponding author.
** Corresponding author at: State Key Laboratory of Environmental Chemistry and Ecotoxicology, Research Center for Eco-Environmental Sciences, Chinese Academy of Sciences, Beijing 100085, China
E-mail addresses: p.zhang.1@bham.ac.uk (P. Zhang), binzhao@rcees.ac.cn (B. Zhao).

https://doi.org/10.1016/j.nantod.2020.100977
1748-0132/© 2020 The Author(s). Published by Elsevier Ltd. This is an open access article under the CC BY-NC-ND license (http://creativecommons.org/licenses/by-nc-nd/4.0/).

considerable attention due to their putative anti-cancer properties and potency in drug delivery [6,7]. Therefore, the risk of human exposure to ZnO NPs through inhalation, ingestion and dermal contact is increasing.

Concern regarding the potential for adverse effects of ZnO NPs on the brain following uptake has been increasing recently. An early study reported that inhalation of micron-sized ZnO particles, generated during welding of galvanized zinc-coated steel, causes impairment of brain function (psycho-organic syndrome) [8]. NPs may enter the brain *via* several routes. For example, inhaled NPs might be transferred to the central nervous system (CNS) *via* the trigeminal nerve after passing the olfactory epithelium [9], or enter the brain directly through axonal transport along the olfactory nerve [10]. A recent study by Chen et al. showed that tongue-instilled ZnO NPs can be transported into the CNS *via* the taste nerve translocation pathway [11]. ZnO NPs ingested or inhaled may reach the systemic blood circulation from the lung or gastrointestinal tract and cause Zn deposition in the brain after crossing the blood-brain barrier [12], and subsequently stimulate oxidative stress and inflammatory responses that cause damage to crucial functional brain regions [13] and consequently lead to neurological disorders.

Given the potency of these multiple portals of entry for ZnO NPs into the CNS, there is a high possibility that exposure to ZnO NPs may cause Zn accumulation in the brain and consequently lead to neurological disorders; however, such data are still limited. A recent *in vitro* toxicological study using primary astrocytes isolated from postnatal 0–2 day old rat pups provided evidence that ZnO NPs have neurotoxic potential [14]. Using an isolated *ex vivo* brainstem-spinal cord prepared from neonatal rats, Nicolosi et al. found that ZnO NPs can exert deleterious effects on the central neural networks responsible for mammalian respiratory rhythm generation [15]. An *in vivo* study showed that orally administered ZnO NPs (30–40 nm) caused deficits in normal motor function in Swiss albino mice [16]. Intranasally instilled ZnO NPs (19.61 ± 5.83 nm) induced Zn deposition in different brain regions of rats including the olfactory bulb, hippocampus, striatum, and cerebral cortex, leading to pathological changes in the brain [17]. Although these pioneering studies provide evidence that ZnO NP exposure can cause Zn accumulation in the brain and result in neurotoxicity, the underlying molecular mechanism remains unclear. Moreover, the origin of the neurotoxicity, *i.e.* whether the toxicity is derived from the particulate form of ZnO or from Zn^{2+} released from ZnO NPs is unknown. Addressing these questions is fundamentally important to the risk assessment and further safe-by-design of ZnO NPs.

With this motivation, ZnO NPs were intranasally administered *via* a single dose to four-week-old male Sprague-Dawley rats, with $ZnSO_4$ as a comparison. The hippocampus was found to be the main target region of Zn deposition for both ZnO NPs and $ZnSO_4$ treatments. Changes to the hippocampal region at mRNA, protein and metabolite levels were analyzed by a combination of transcriptomics, proteomics and metabolomics techniques. Cholinergic neurotransmission was found to be the main pathway affected and the mechanisms were then explored. The contribution of ZnO dissolution to the observed biological effects was also explored to identify the origin of the toxicity. This study provides new understanding of the impact of ZnO NPs on the brain and highlights a basis for safe-by-design of ZnO NPs.

Results and discussion

ZnO NP exposure caused Zn accumulation and pathologies in the brain

In a previous study, Liu et al. [17] used a dose of 20 mg/kg BW for acute inhalation exposure study and found ZnO NPs caused neurotoxicity to Wistar rat. In our study, we tested three lower doses 4.33, 8.67 and 13 mg Zn/kg BW in preliminary experiments to find dose for the subsequent studies. A decrease of body weight was observed only in the high dose (13 mg Zn/kg BW) treatment (Fig. S1). In addition, we found that the dose of 13 mg Zn/kg BW caused sufficient Zn accumulation in the brain (Fig. S2) for detection by XAFS with a good signal for chemical species analysis to allow confirmation of the Zn form, which was a core goal of the present study in order to correlate speciation with biological effect. Therefore, 13 mg Zn/kg BW was used for the following studies.

Intranasal exposure to ZnO NPs (30 ± 6 nm; Fig. S3) at a single dose (13 mg/kg BW) did not cause significant change in brain weights and relative brain weights (brain weights / body weights) determined at 7 days post-exposure, while $ZnSO_4$ exposure induced a slight decrease in the relative brain weights ($p < 0.01$) (Fig. S1).

Zn content was determined across critical functional brain regions. ZnO NP exposure led to significant Zn accumulation (20 % increase as compared with untreated control) only in the hippocampus ($p < 0.01$; Fig. 1a) while $ZnSO_4$ exposure caused significant Zn elevation in several brain regions including the hippocampus, cerebellum and midbrain ($p < 0.01$; Fig. 1a). Additionally, the amount of newly accumulated Zn in the hippocampus was similar in both the ZnO NP and $ZnSO_4$ groups. There was no significant accumulation of Zn in other brain regions after either treatment ($p > 0.05$; Fig. 1a). Zn accumulated in the hippocampus after both treatments, indicating that the hippocampus was the main target region, which is consistent with previous studies that also found the hippocampus as the main target region after intranasal administration of ZnO [17], Fe_2O_3 [18] or TiO_2 NPs [19]. For example, TiO_2 NPs had significantly accumulated in the hippocampus only 2 days after intranasal exposure and the Ti content was much higher than in other regions such as the olfactory bulb, cerebral cortex and cerebellum after 30 days of exposure (with NP administration every other day). It was suggested that after NPs enter the brain, the olfactory bulb is the first deposition region, followed by the hippocampus and other sub-brain regions with prolonged exposure time [19]. In our study, although the Zn content in olfactory bulb did not show significant difference between treatment and control groups, it showed a trend of increase for both ZnO NPs (7.42 %) and $ZnSO_4$ (7.37 %). The reason might be due to that the background Zn content in brain is very high relative to the newly accumulated Zn. Such slight difference between endogenous and exogenous element cannot be distinguished by inductively coupled plasma optical emission spectrometry (ICP-OES) and needs other techniques such as isotope labeling [20]. Such phenomenon was also reported in a previous study where the authors also found the trend of Zn accumulation in olfactory bulb with no statistical significance after daily exposure to 20 mg/kg BW intranasally instilled ZnO NPs for 15 days [17]. The exact regions and amounts of NP deposition in brain depend on factors such as the physicochemical properties of the NPs and the exposure mode, animal species and duration. Since ZnO NPs and $ZnSO_4$ resulted in similar amounts of Zn accumulation in the hippocampal region, comparing the effects of ZnO NPs with that of $ZnSO_4$ will provide insights into the mechanism of action of ZnO NPs. Thus, further analyses focused on the hippocampal region.

The Zn species in the hippocampus were analyzed by synchrotron radiation-based X-ray fine structure spectroscopy (XAFS) (Fig. 1b). The Zn K-edge XAFS spectra showed similar features between control and treatment groups indicating that similar species were present. Linear combination fitting (LCF) analysis demonstrated that Zn in both ZnO NP and $ZnSO_4$ groups presented the same form as that in the control samples, that is, Zn complexes, suggesting no presence of particulate ZnO in the hippocampus from ZnO NP-instilled animals. This indicated that any effects occurring

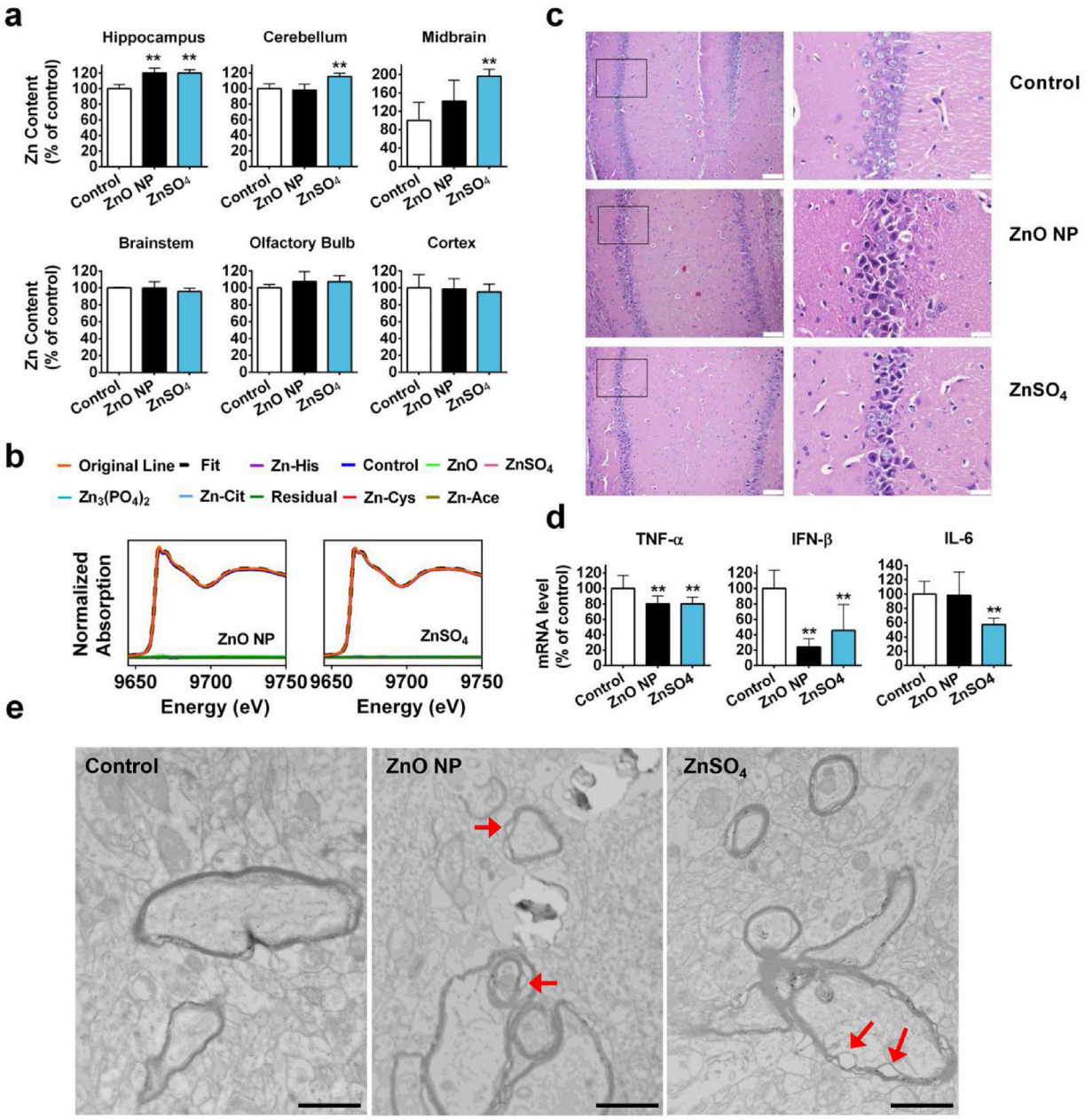

Fig. 1. ZnO NP exposure induced Zn accumulation in the brain and caused pathological changes in the hippocampus. (a) Zn contents in different brain regions following ZnO NP or $ZnSO_4$ exposure (n = 6). $^{**}p < 0.01$ indicates significant difference as compared with control. (b) XAFS spectra of hippocampal samples from ZnO NP or $ZnSO_4$ treated animals. Control in the XAFS spectra indicates the spectrum collected from the hippocampal samples of the untreated control animals; Zn-His, Zn-Cys, Zn-Cit, and Zn-Ace indicate Zn-histidine, Zn-cysteine, Zn-citrate, and Zn-acetate complexes, respectively; original line indicates originally collected XAFS spectra; fit indicates the fitting spectra by Linear Combination Fitting (LCF) analysis. (c) Histopathological analysis of the hippocampus. Sections were stained with H&E, and the images are representative of all sections examined. Images in the right column are the magnification of the rectangle areas highlighted in the left column; scale bar = 100 μm (left) and 20 μm (right). (d) Expression levels of TNF-α, IFN-β, and IL-6 determined by real-time PCR analysis of total RNA extracted from the hippocampus of animals from different treatment groups. (e) TEM images of the hippocampal region. Red arrow indicates vacuolate-like structure; scale bar = 1 μm.

in this region in the ZnO NP group were induced by the Zn^{2+} dissolved from ZnO NPs.

Hematoxylin and eosin (H&E) staining showed pathological changes in the hippocampus, with shrunken hyperchromatic nuclei in both ZnO NP and $ZnSO_4$ groups (Fig. 1c). Proinflammatory cytokines are important modulators of neural functions and neuronal survival [21]. Our data showed that transcript levels of TNF-α significantly decreased by 20 % in both treatment groups. IFN-β decreased by 75 % and 55 % in ZnO NP and $ZnSO_4$ groups, respectively. IL-6 was only downregulated in the $ZnSO_4$ group. These results indicated that release of proinflammatory cytokines may be decreased in the hippocampus of treated animals (Fig. 1d). TEM images showed the appearance of vacuole-like structures in myelinated nerve fibers in both ZnO NP and $ZnSO_4$ groups (Fig. 1e), indicating separation of the myelin sheath and damaged lamellar structures. All these data suggested that ZnO NP exposure caused pathological changes in brain.

ZnO NP exposure induced disturbance in cholinergic neurotransmission

To reveal the holistic molecular consequences and identify the key affected pathways linked with the observed pathologies, a combination of omics techniques was employed. Omics technologies

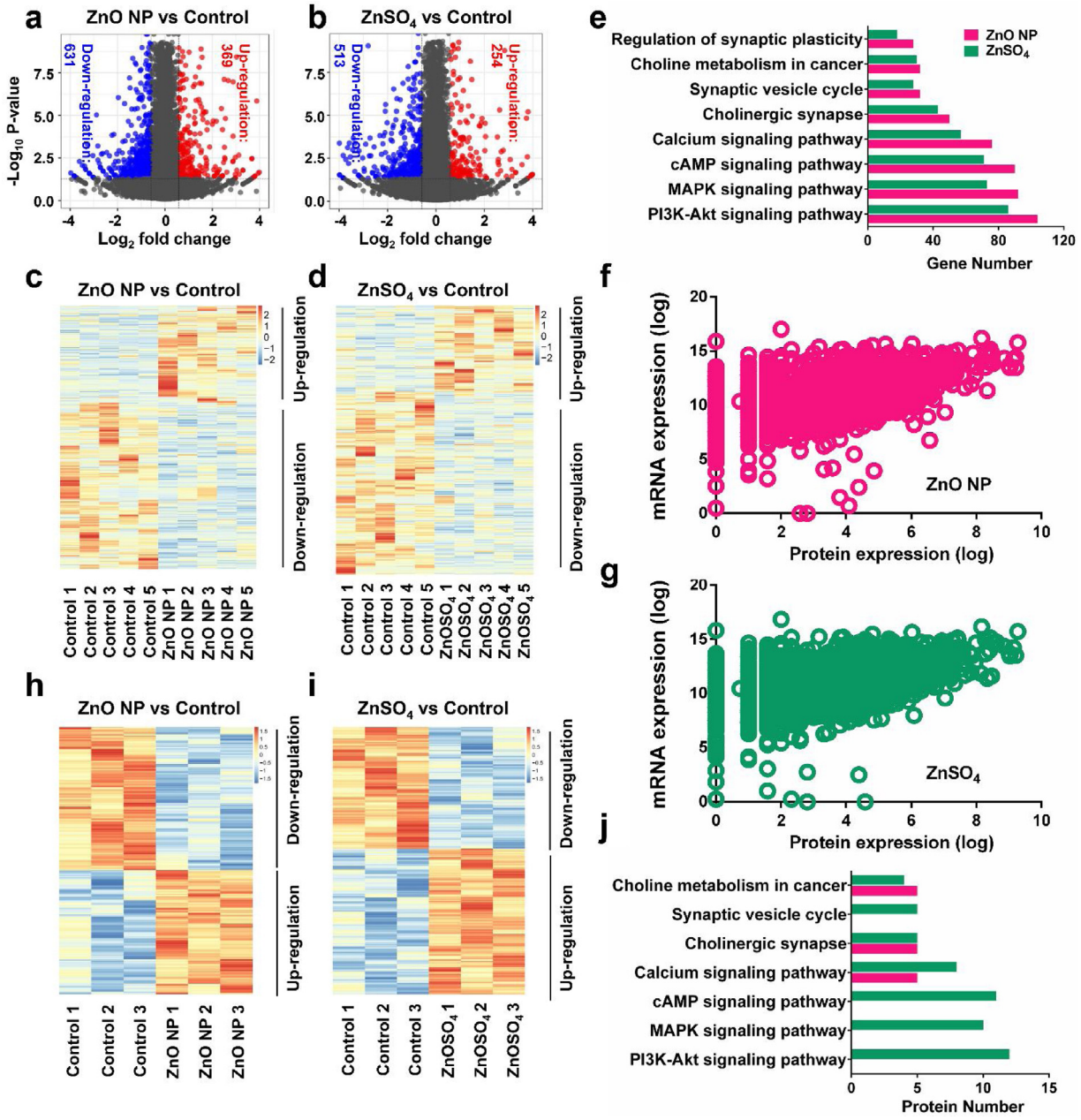

Fig. 2. Transcriptomic and proteomic data showed that cholinergic neurotransmission was the main target of ZnO NP action. (a-b) Volcano plots of the transcriptomic results following ZnO NP (a) or $ZnSO_4$ exposure (b). n = 5. (c-d) Heatmap analysis of significantly differentially expressed genes in response to ZnO NPs (c) or $ZnSO_4$ (d). (e) KEGG enrichment analysis of differentially expressed genes in ZnO NP and $ZnSO_4$ groups. (f-g) Correlations between mRNA levels and protein levels in ZnO NP (f) or $ZnSO_4$ group (g). (h-i) Heatmap analysis of significantly differentially expressed proteins in response to ZnO NPs (h) or $ZnSO_4$ (**i**). n = 3. (j) KEGG enrichment analysis of differentially expressed proteins in the ZnO NP and $ZnSO_4$ groups.

have opened new avenues in many fields including toxicological and pathogenetic and pathophysiological studies, enabling us to build a molecular basis for the connection between environmental factors and different diseases [22,23]. We firstly assessed genome-wide gene expression by transcriptomic RNA sequencing (RNA-seq) analysis of total mRNA isolated from the corresponding hippocampal samples. The volcano plots of the transcriptomics showed 23,413 genes expressed (Table S1) in the ZnO NP treatment group, with 631 significantly downregulated and 369 upregulated ($p < 0.05$ and $|\log_2 FC| > 0.59$) compared to the unexposed control (Fig. 2a). For the $ZnSO_4$ group, of the 23,453 expressed genes (Table S1), 513 were significantly downregulated and 254 were significantly upregulated (Fig. 2b). Fig. 2c and d show the heatmaps of the differentially expressed genes in the ZnO NP and $ZnSO_4$ exposed groups, respectively. Significant differences can be observed between the different treatments, with intragroup parallelism.

Gene set enrichment analysis (GSEA) using the KEGG (Kyoto Encyclopedia of Genes and Genomes) database showed that the differentially expressed genes triggered by ZnO NP exposure were significantly enriched in biological processes including cholinergic synapse, choline metabolism, synaptic vesicle cycle, and intracellular signaling pathways triggered by nicotinic acetylcholine receptor (nAChR) including the PI3K-Akt, MAPK, cAMP, and calcium signaling pathways, indicating that the cholinergic neurotransmission pathway was disturbed (Fig. 2e). Cholinergic synapses use acetylcholine (ACh) as their neurotransmitter for signal transmission. During neurotransmission, ACh is exocytosed from synaptic vesicles and released into the synaptic cleft, where it can activate both

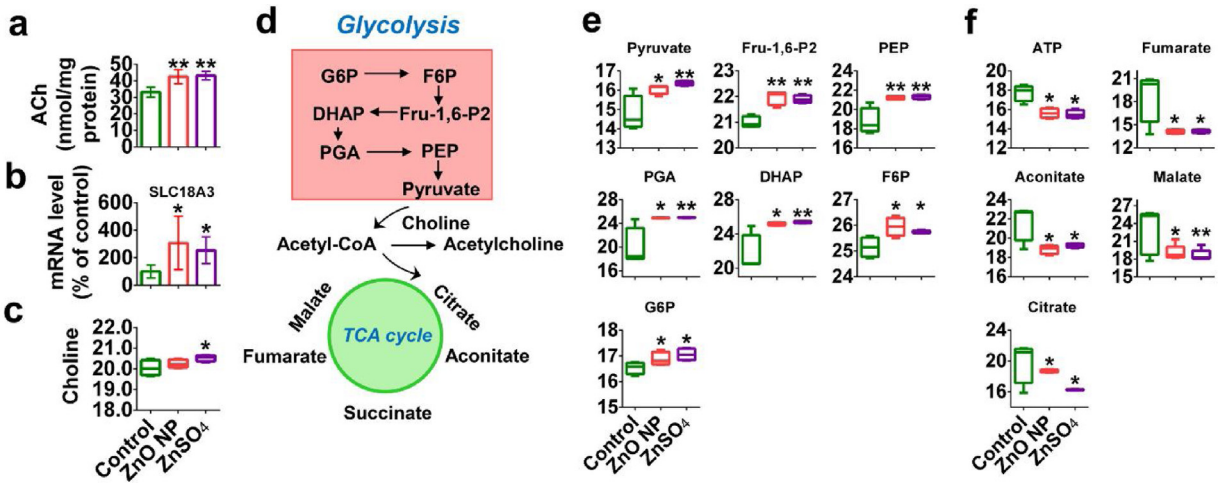

Fig. 3. ZnO NP exposure enhanced ACh release. (a) Intracellular ACh levels in the different treatment groups. (b) Relative expression level of SLC18A3. (c) Box plots of relative abundance of choline. (d) Schematic figure showing intermediates related to the biosynthesis of ACh. (e-f) Box plots of the relative abundance of metabolites related to the biosynthesis of pyruvate (e) and metabolism of acetyl-CoA (f). Abbreviation: Glucose 6-phosphate: G6P; fructose 6-phosphate: F6P; fructose 1,6-bisphosphate: Fru-1,6-P2; dihydroxyacetone phosphate: DHAP; 3-phosphoglycerate: PGA; phosphoenolpyruvate: PEP. n = 10; $^{*}p < 0.05$ and $^{**}p < 0.01$ indicate significant difference as compared with control.

muscarinic acetylcholine receptors (mAChRs) and nAChRs, triggering a downstream signaling cascade, ultimately modulating cellular response or synaptic plasticity [24]. Cholinergic synaptic neurotransmission can be terminated following rapid hydrolysis of ACh at the synaptic cleft by the enzyme acetylcholinesterase (AChE). Here, for the first time we have discovered that ZnO NPs can disturb cholinergic neurotransmission in the hippocampus, which may potentially alter hippocampal synaptic plasticity or modulate cellular response [25]. Similarly, $ZnSO_4$ exposure also caused changes in those abovementioned pathways and processes (Fig. 2e), indicating that the molecular consequences induced by ZnO NP exposure were similar to those induced by $ZnSO_4$.

We next carried out quantitative proteomic analysis to study the holistic protein changes in the hippocampus. Overall, the absolute ("static") levels of proteins correlated positively with mRNA transcript levels in both ZnO NP (Spearman coefficient $r_s = 0.21$) (Fig. 2f) and $ZnSO_4$ (Spearman coefficient $r_s = 0.2168$) groups (Fig. 2g). No correlations were observed between the changes in mRNA transcript levels and the changes in protein levels at the level of the whole datasets (Fig. S4), consistent with the very different processes and timescales for regulation of genes and proteins which requires detailed temporal data to deconvolute. Such a phenomenon was also reported previously [26], arising from differential regulation of mRNA expression, stability, and degradation as compared with protein expression, stability, and degradation [27]. We detected 6008 proteins in all samples (Table S2), and of these, 338 and 433 were differentially regulated in the ZnO NP and $ZnSO_4$ groups, respectively. As shown in the heatmap (Fig. 2h and i), excellent intragroup parallelism and intergroup differences were noted. ZnO NPs and $ZnSO_4$ induced similar changes in protein pattern. Consistent with the transcriptomic results, the differentially expressed proteins induced by ZnO NPs or $ZnSO_4$ were also enriched in pathways related to cholinergic neurotransmission such as cholinergic synapse and choline metabolism (Fig. 2j), further demonstrating at protein level that cholinergic neurotransmission was the main pathway affected by ZnO NP and $ZnSO_4$ exposure. The signaling pathways triggered by nAChR, such as the PI3K-Akt signaling pathway, the MAPK signaling pathway and the cAMP signaling pathway, were enriched only in the $ZnSO_4$ group (Fig. 2j), indicating that the effect of ZnO NPs on the cholinergic system at the protein level is not as significant as that of $ZnSO_4$ or as significant as the effects that occurred at transcript levels, although the Zn accumulation in the hippocampus was similar. This may be due to the fact that in the $ZnSO_4$ group Zn ions were instantaneously available, producing a rapidly elevated local concentration of Zn^{2+}, while in the ZnO NP group, dissolution of the ZnO NPs took time and the rate of the release of Zn ions is not comparable with $ZnSO_4$. For example, only 0.44 % and 0.1 % of Zn^{2+} can release from ZnO NPs in water and in 0.1 % in sodium carboxymethyl cellulose solution (SCMC) which was also used in this study as a stabilizer, respectively, after 48 h incubation [22].

Taken together, the transcriptomic and proteomic data showed that cholinergic neurotransmission is the main pathway affected by ZnO NP or $ZnSO_4$ exposure. This indicated that the cholinergic system is a molecular target of ZnO NP action in the brain, and that Zn^{2+} ions released from the ZnO NPs are the main contributor.

ZnO NP exposure enhanced ACh release by upregulating the ACh transporter and promoting ACh synthesis

Since cholinergic neurotransmission uses ACh as the neurotransmitter, ACh release in the hippocampal region was examined next. Intracellular ACh levels were found to be enhanced in both ZnO NP and $ZnSO_4$ treatments ($p < 0.01$; Fig. 3a), further demonstrating the enhanced cholinergic neurotransmission. Vesicular acetylcholine transporter (VAChT) is responsible for loading ACh into secretory organelles in neurons thus making ACh available for secretion. Previous research has shown that VAChT stringently regulates ACh release and is proposed as a possible target to enhance cholinergic function. Upregulation of VAChT is sufficient to lead to increased ACh release [28]. The mRNA levels of its encoding gene, solute carrier family 18, member 3 (SLC18A3), were found to be significantly upregulated in both treatment groups ($p < 0.05$; Fig. 3b). This suggested that the upregulation of VAChT might be a potential mechanism leading to the enhanced ACh release detected.

ACh is synthesized from acetyl coenzyme A (acetyl-CoA) and choline by the enzyme choline acetyltransferase. We found that the choline level was significantly elevated in the $ZnSO_4$ group ($p < 0.05$) and showed a slight increasing trend ($p > 0.05$) in the ZnO NP exposed group (Fig. 3c). One of the sources of choline used for ACh synthesis comes from the breakdown of phosphatidylcholine [29]. The increased choline reserves ensure a rich supply of precursors that can be directed into ACh.

Since glucose-derived pyruvate metabolism is a principal source of acetyl-CoA in the brain as shown in the schematic in Fig. 3d, we quantified pyruvate and intermediates related to the synthesis

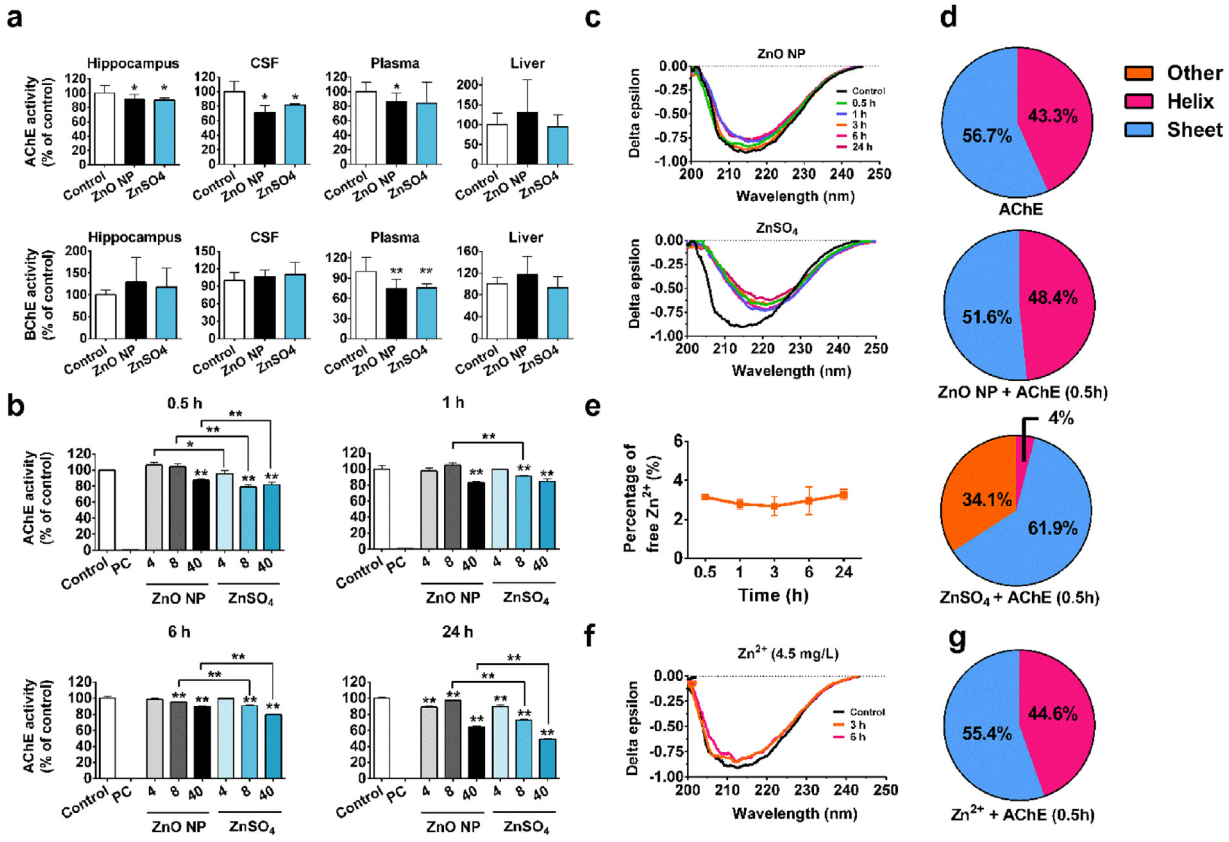

Fig. 4. Effects of ZnO NPs and $ZnSO_4$ on enzymatic activity and secondary structure of AChE. (a) AChE and BChE activity in hippocampus, CSF, plasma, and liver (n = 10). $^{*}p < 0.05$ and $^{**}p < 0.01$ indicate significant difference compared with unexposed control animals. (b) AChE activity in lysate of hippocampal tissues after incubation with ZnO NPs, $ZnSO_4$, BW284c51 (AChE inhibitor used as the positive control (PC)), or with 0.1 % SCMC (negative control) for 0.5 h, 1 h, 6 h, 24 h. $^{*}p < 0.05$ and $^{**}p < 0.01$ indicate significant difference compared to control. (c) CD spectra of AChE after incubation with ZnO NPs or $ZnSO_4$ for 0.5 h to 24 h. (d) Effects of ZnO NPs or $ZnSO_4$ on the fractional contents of secondary structure components of AChE after incubation with ZnO NPs or $ZnSO_4$ for 0.5 h. (e) Percentage of free Zn^{2+} dissolved from ZnO NPs after 0.5 h to 24 h incubation with AChE *in vitro*. (f) CD spectra of AChE after incubation with Zn^{2+} (4.5 mg/L, with amount equal to that obtained in e). (g) Change in secondary structure of AChE after interaction with dissolved Zn^{2+} in e.

of pyruvate. We found pyruvate concentrations in the hippocampus were elevated by 111 % and 157 % in ZnO NP ($p < 0.05$) and $ZnSO_4$ treatment ($p < 0.01$), respectively, compared to untreated controls (Fig. 3e). We also observed that the glycolytic intermediates involved in the biosynthesis of pyruvate, including glucose 6-phosphate (G6P), fructose 6-phosphate (F6P), fructose 1,6-bisphosphate (Fru-1,6-P2), dihydroxyacetone phosphate (DHAP), 3-phosphoglycerate (PGA), and phosphoenolpyruvate (PEP) were all significantly increased in both treatments (Fig. 3e). The increased glycolytic substrate levels may ensure a rich supply of substrates that flux into pyruvate. Moreover, we found that intermediates in the TCA (tricarboxylic acid cycle) cycle, for which acetyl-CoA serves as a direct energy precursor substrate, including citrate, aconitate, fumarate, malate, and ATP, were all decreased following treatment (Fig. 3f), suggesting a reduction in the flux of acetyl-CoA to the TCA cycle to ensure that more acetyl-CoA can fuel the ACh pool. These data suggested that enhanced ACh synthesis is another potential mechanism leading to the increased release of ACh. The $ZnSO_4$ treatment group presented similar effects on ACh transporter and precursors for ACh synthesis as occurred in the ZnO NP group, suggesting that Zn^{2+} ions released from the ZnO NPs were the main contributor to the observed effects.

ZnO NP exposure enhanced ACh release by suppressing hippocampal AChE activity

AChE is a fundamental enzyme for cholinergic neurotransmission, which can hydrolyze ACh to terminate synaptic transmission. Therefore, alteration of AChE activity can directly affect ACh levels. AChE activity has also been reported to be associated with neurological disorders such as Alzheimer's disease (AD). For example, previous evidence showed that AD patients or patients with probable Alzheimer-type dementia showed significant reduction of AChE activity in lumbar cerebrospinal fluid (CSF) [30] and in the hippocampus [31], while other results showed increased plasma AChE activity in subjects with AD [32]. We found that the AChE activity in the hippocampus and CSF were significantly suppressed in both ZnO NP and $ZnSO_4$-treated animals ($p < 0.05$; Fig. 4a). Suppressed AChE activity can delay or inhibit the degradation of ACh in the synaptic cleft, thereby exacerbating the accumulation of ACh. This result demonstrated that suppression of AChE activity is another potential mechanism leading to upregulated ACh levels in the hippocampus. In addition to AChE, the levels of ACh are also regulated by butyrylcholinesterase (BChE). Our results did not show significant change in enzymatic activity of BChE in the hippocampus and CSF in both treatments ($p > 0.05$). We also examined the activity of the two enzymes in plasma. We found significantly decreased AChE activity in plasma of $ZnSO_4$ exposed animals ($p < 0.05$) and reduced BChE activity in plasma of both groups ($p < 0.01$) (Fig. 4a). Low plasma cholinesterase activities were reported to be associated with AD [33]. Plasma cholinesterase originates mostly from the liver [34]. However, we found that cholinesterase activity in the liver did not show any change in response to either treatment (Fig. 4a).

Mechanisms involved in the suppressed AChE activity by ZnO NP exposure

Zn^{2+} released from ZnO NPs inhibited AChE activity, possibly by interacting with its structure

Given the fundamental roles of AChE in cholinergic neurotransmission, the mechanisms involved in the suppression of AChE activity by ZnO NP exposure were further explored. In general, the activity of AChE can be inhibited either by direct interaction with its structure or through suppression of transcription. For example, organophosphorus insecticides (OP) can irreversibly inhibit the activity of AChE by binding to its catalytic residue [35], while 2,3,7,8-tetrachlorodibenzo-p-dioxin (TCDD) can exert a suppressive effect in neuronal AChE through transcriptional regulation [36]. *In vitro* assays were employed to investigate the possibility that direct interaction of ZnO NPs with AChE affects the enzymatic activity of AChE. ZnO NPs (with Zn concentrations of 4, 8 or 40 mg/L) were mixed with lysate of hippocampal tissues for different durations. Results showed that AChE activity was inhibited by ZnO NPs in a time- and concentration- dependent manner. ZnO NPs of 40 mg/L started the inhibition of AChE activity after 0.5 h, and stronger inhibition was found over time, with 35 % inhibition after 24 h. While at low concentration (4 mg/L), ZnO NPs started depressing the activity of AChE after 24 h of incubation (Fig. 4b). Compared with ZnO NPs, $ZnSO_4$ with same molar concentration of Zn induced stronger inhibition at all concentrations tested at all time points (Fig. 4b, $p < 0.05$). These data indicated that $ZnSO_4$ is a stronger inhibitor of AChE than ZnO NPs. It was previously reported that the dissolution of ZnO NPs under aqueous conditions is low, and increases with the presence of biological components such as amino acids and peptides [37] as well as under acidic conditions [38]. Therefore, the different inhibition rates between the two treatment groups in the *in vitro* assay may be due to the lower Zn^{2+} release rate from ZnO NPs compared to the instantaneously available Zn^{2+} from $ZnSO_4$. Our *in vivo* data showed Zn accumulation in the hippocampus was similar between the two treatment groups (Fig. 1a), and AChE activity in the hippocampus did not show a significant difference between the two treatment groups (Fig. 4a), further demonstrating that Zn^{2+} contributes to the AChE inhibition.

The enzymatic activity of an enzyme is determined by its structure. We further examined if direct interaction of ZnO NPs with AChE can cause conformational change. We acquired circular dichroism (CD) spectra of AChE after incubation with ZnO NPs or $ZnSO_4$ for different durations. $ZnSO_4$ caused significant peak shift of the original spectra of AChE (from 214.7 nm to 220.6–222.5 nm) while ZnO NPs had no effect on the peak position (Fig. 4c). The compositions of the secondary structure of AChE with or without the presence of ZnO NPs or $ZnSO_4$ are presented in Fig. 4d. Both α-helix and β-sheet content showed no significant changes after incubation with ZnO NPs for 0.5 h (Fig. 4d). However, the addition of $ZnSO_4$ significantly decreased the α-helix content and increased the β-sheet and random coil contents after 0.5 h incubation (Fig. 4d). There were no further changes with longer incubation times. These data indicate that Zn^{2+} can cause structural perturbation of the enzyme. Although the structural region that was affected could not be determined from the CD data, the possibility that the catalytic region was perturbated cannot be ruled out. As a result, the function of the enzyme might be reduced due to inactivation of the catalytic residue.

Further experiments found that the Zn^{2+} released from the ZnO NPs after incubation with AChE only accounted for 3% of the total Zn after 0.5 h–24 h incubation (Fig. 4e). Those released Zn^{2+} did not show any effect on the CD spectra (Fig. 4f) and the fractional contents of secondary structure types (Fig. 4g). This indicated that the amount of Zn^{2+} released from the ZnO NPs is not sufficient to cause any change in the secondary structure of AChE. As described above, however, ZnO NP dissolution is higher in the presence of biological components as present *in vivo*, and the released Zn^{2+} was sufficient to induce structural changes of AChE and subsequently caused suppression of the enzyme activity.

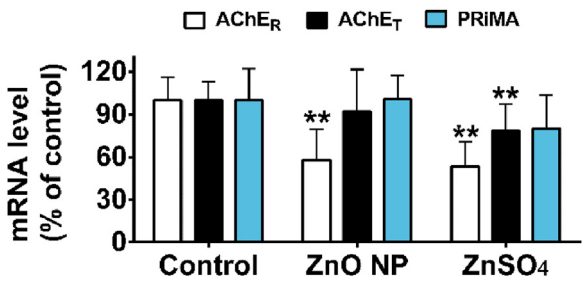

Fig. 5. Expression levels of AChE transcripts ($AChE_R$ and $AChE_T$ variants) and PRiMA transcripts in the hippocampus of ZnO NP or $ZnSO_4$-treated animals. n = 10; $^{**}p < 0.01$ indicates significant difference compared with control.

Transcriptional down-regulation mechanism as a potential mechanism for suppression of AChE activity

In order to determine if the decrease in hippocampal AChE activity was a consequence of transcriptional regulation, we also measured the expression of AChE at mRNA level. AChE is expressed as multiple splice variants, which serve both cholinergic degradative functions and non-cholinergic functions [39]. The results showed that the levels of the non-cholinergic "readthrough" AChE ($AChE_R$) decreased by 42 %; while $AChE_T$ (cholinergic "tailed" variant), the most abundant variant of AChE in the human brain, did not show any significant change in transcript levels in the hippocampus of ZnO NP-treated animals (Fig. 5). For $ZnSO_4$ treated animals, $AChE_R$ and $AChE_T$ transcript levels significantly decreased by 46 % and 21 %, respectively ($p < 0.01$). The proline-rich membrane anchor (PRiMA-1), a structural subunit of the active form of neuronal AChE, did not show significant change at the mRNA level in either treatment (Fig. 5). Decrease in the mRNA expression of AChE subunit resulted in decreased expression of the active form of AChE, which may lead to decreased AChE activity. These findings suggest that transcriptional down-regulation might be a potential mechanism for the suppression of AChE activity. Future studies are necessary to explore the mechanism, *e.g.*, the transcription factors involved in the down-regulation process.

Implications for neurological disorders

The importance of Zn to the function of the CNS is undisputable, given its structural and catalytic functions in proteins, transcription factors and enzymes that regulate a breadth of cellular processes and intracellular signaling transduction essential for brain function, as well as its vital role as the free ionic form in modulating synaptic function [40,41]. While Zn is indispensable for physiological brain functions, excess brain Zn content can also induce a myriad of pathological conditions, ultimately leading to the onset of chronic neurological disorders such as Alzheimer's disease (AD), epilepsy, and Parkinson's disease [42–44]. Thus, maintaining Zn at homeostatic levels is crucial for normal brain development and function. Taking exogenous Zn supplementation from food and vitamins is considered the most common cause of zinc excess. However, only limited amounts of orally ingested Zn can reach the brain since humans have the capacity to maintain relatively constant tissue levels of Zn *via* the gastrointestinal system, except under extremes of intake. Besides, following uptake of Zn into enterocytes and subsequent transport from enterocytes to the blood, approximately 98.3 % of zinc is distributed to tissues including skeletal muscle,

bone, skin and liver, while only a very small amount of Zn can enter the brain by crossing the blood-brain barrier system [45]. Unlike dietary Zn intake, inhaled Zn can enter the brain through multiple pathways without gastrointestinal adjustments.

As we found in this study, inhalation of ZnO NPs resulted in Zn overaccumulation in the hippocampus and caused brain pathologies and disturbance of cholinergic neurotransmission in the hippocampus which are typical of those found in patients with AD or AD-type diseases. In addition, increasing evidence in recent years suggests that demyelination of neurons is mechanistically important in AD pathology [46]. The structural changes of myelinated nerve fibers observed in our study may imply the potential for subsequent development of AD. The elevated glutamate levels in the hippocampus further demonstrate the potential of ZnO NPs to induce AD (Fig. S5). Glutamate is another common neurotransmitter in the brain, and in the brains of AD patients excessive glutamate can release due to the death of brain cells [47], which can overstimulate healthy brain cells and cause further damage to the brain. Taken together, our findings give implication that ZnO NP-induced Zn accumulation and alterations in cholinergic neurotransmission in brain might be linked with chronic neurological disorders such as AD. Further studies are required to provide more evidence for this link and explore the involved mechanism. Moreover, previous study has shown that high dose of oral administered TiO_2 NPs also caused suppression of AChE activity and increased level of cerebral IL-6 in brain, suggesting that other NPs may also cause neuroinflammation and neurotoxicity [48]. While the TiO_2 NPs might induce neurotoxicity *via* different mechanism given the difference in composition and solubility compared with ZnO NPs, further studies are therefore also needed to determine the potential of other NPs for inducing neurotoxicity.

Conclusion

In conclusion, ZnO NP exposure caused significant Zn accumulation in the hippocampus and induced pathological changes and a cascade of signaling effects related to cholinergic neurotransmission. ZnO NPs increased the release of neurotransmitter ACh by enhancing ACh synthesis or transportation or by inhibiting the activity of AChE. ZnO NPs suppressed AChE activity, possibly due to the interaction of Zn^{2+} released from the ZnO NPs with AChE altering its secondary structure or *via* a transcriptional down-regulation mechanism. The excessive Zn accumulation and consequent disturbance of cholinergic neurotransmission in the brain indicate that inhalation of ZnO NPs may be a risk factor for neurological disorders such as AD. Further studies are thus required to explore the key molecular initiating events and consequences such as effects on brain function and neurological behavior over longer term and multiple exposures to ZnO NPs. Additionally, the reversibility potential of the ZnO NPs induced neurotoxicity need to be explored in the future research. The finding that Zn^{2+} released from ZnO NPs was the main contributor to the observed biological effects provides a basis for safe-by-design of ZnO NPs.

Experimental section

Animal Experiment: Animal procedures were permitted by, and conducted in accordance with, Chinese Academy of Science Animal Care guidelines and ARRIVE guidelines. Four-week-old male Sprague-Dawley rats were housed 2 animals/cage in a 12 -h light/dark cycle with food and water *ad libitum*. After 7 days' acclimatization, rats (mean weight 194 ± 10 g) were randomly divided into three groups of thirty and instilled intranasally with one single dose (13 mg Zn/kg BW) of ZnO NPs or $ZnSO_4$. On the day of instillation, ZnO NPs and $ZnSO_4$ were dispersed / dissolved, respectively, in 0.1 % SCMC to achieve Zn elemental concentration of 64 mg/mL. A total of 40 μL of the suspensions were administered intranasally to rats, 10 μL at a time, alternating between each naris every 2 min. This provided a total dosage of 13 mg Zn/kg BW in both treatments. Rats were also exposed to 0.1 % SCMC as a control. Rats were left undisturbed until 7 days post exposure, when they were sacrificed after being anesthesized in an isoflurane-filled chamber. Brains were collected immediately and samples from different brain regions were dissected and washed 3 times with 1 × PBS, and then snap-frozen in liquid nitrogen and stored at −80 °C for futher study.

Zn Content and Chemical Speciation: Zn concentrations were measured on a Perkin Elmer Optima 8000 inductively coupled plasma optical emission spectrometry (ICP-OES) (Perkin Elmer, Shelton, CT, USA). Zn chemical species was analyzed using XAFS. A detailed description of the sample preparation and the quality control procedures are provided in the SI.

Histopathological Examination: Brain tissues were washed with 0.9 % cold saline and fixed in 2.5 % glutaraldehyde polyoxymethylene solution. Briefly, the samples were dehydrated and embedded in paraffin wax and sliced at a thickness of 4 μm using a microtome. The sections were subjected to three consecutive xylene washes to remove paraffin and were subsequently hydrated with five consecutive ethanol washes in descending order of concentration: 100 %, 95 %, 80 %, 70 %, and deionized water. The paraffin sections were then stained with H&E, and pathological changes were visualized using a light microscope with Leica Application Suite software (Leica Microsystems). Five sections were examined from each animal, and six animals were evaluated from each group.

Transmission Electron Microscopy (TEM): Small blocks (~1 mm^3) of brain tissue (n = 6) were fixed for 2 h. Then, the samples were dehydrated through an ethanol gradient and embedded in Epon resin. The blocks were then sectioned on a microtome and the ultrathin sections (100 nm) obtained were mounted on copper grids. Ultrastructural examination and photography were performed on a Bio TEM (JEOL 1400, Toyko, Japan).

Omics Analysis: RNA-seq analysis was performed using a BGIseq500 platform (BGI-Shenzhen, China). Quantitative proteomic analysis was carried out using liquid chromatography-tandem MS (LC–MS/MS). Hydrophilic interaction chromatography (HILIC) triple quadrupole (QqQ) tandem mass spectrometry (MS/MS) was used for targeted metabolomic analysis. Detailed information is provided in Section 1 of the SI.

Quantification of Intracellular ACh Release in the Hippocampus: Intracellular ACh release was measured using the Amplex Red detection kit (Thermo Fisher scientific) according to the manufacturer's instructions. Detailed information is provided in Section 1 of the SI.

Determination of AChE and BChE Enzymatic Activity: AChE enzymatic activity was determined according to the method described previously with some modification [49] (Section 1 of the SI).

In Vitro Assay to Examine the Effects of ZnO NPs on AChE Activity: Total protein was extracted from hippocampal tissue as described above. The protein samples were incubated with ZnO NP or $ZnSO_4$ solution (with Zn concentrations of 4, 8, and 40 mg/L) for 0.5 h, 1 h, 6 h, and 24 h. The newly accumulated Zn in hippocampus region measured by ICP-OES was about 4.5 mg/kg for both ZnO and $ZnSO_4$ treatments. Therefore, we used a series of concentration (4, 8, and 40 mg/L) for the *in vitro* studies. SCMC solution was used as the control and BW284c51 (AChE inhibitor) was used as the positive control (PC). AChE activity was then examined using the protocol described above.

Circular Dichroism (CD) Measurements: CD spectra of AChE were measured with an 0.1-cm path length cylindrical cell in the 200−260 nm wavelength region at 25 °C. Briefly, 10 units of AChE enzyme were incubated with ZnO NP or $ZnSO_4$ solution (with Zn

concentration of 150 mg/L) for 0.5, 1, 3, 6 and 24 h. Zn concentration was selected based on a preliminary experiment in which we found that an obvious structural change of AChE can be observed at this concentration. Samples were analyzed with CD spectrophotometry (JASCO International Co., Ltd., Hachioji, Tokyo, Japan). The molar ellipticity was measured every 2 s with an integration time of 100 nm min^{-1}. Full wavelength scans of each sample were performed three times and the average determined for each sample. All the experiments were performed in triplicate. Secondary structure of AChE before and after incubation with ZnO NPs and $ZnSO_4$ was obtained by analyzing the CD spectra on Dichroweb [50].

Dissolution of ZnO NPs after Incubation with AChE: Dissolution of ZnO NPs was analyzed by measuring the Zn^{2+} released into solution. Briefly, ZnO NP suspensions (150 mg/L) were incubated with 10 units of AChE for 0.5 h, 1 h, 3 h, 6 h and 24 h at 37 °C. Samples were taken at different time points and centrifuged at 13,000 rpm for 10 min. The supernatants were collected and diluted with 2% nitric acid for ICP-OES analysis (PerkinElmer, USA). A range of Zn standard solutions (0.1, 1, 5, 10, 50, 100, 500, 1000 μg/L) were used for calibration. The recovery rate of Zn was tested and found to be 99.7 %.

Real-time Quantitative PCR: Total RNA was isolated using Trizol reagent (Invitrogen, Carlsbad, CA, USA). Then cDNA was prepared with 5 μg RNA using Moloney Murine Leukemia Virus Reverse Transcriptase (Invitrogen) according to the manufacturer's instructions. Real-time PCR was performed using SYBR Green Master mix and Rox reference dye according to the manufacturer's instructions (Applied Biosystems, Foster City, CA, USA). The primers used are listed in **Table S3**. The SYBR green signal was detected by MX3005 P multiplex quantitative PCR system (Stratagene, La Jolla, CA, USA). The relative transcript expression levels were quantified using the ΔΔCT method. The specificity of amplification was confirmed by melting curves and by gel electrophoresis.

Statistical Analysis: Data are expressed as mean ± SD and were analyzed with GraphPad InStat software (Version 3, GraphPad Software, Inc., La Jolla, CA). Student's *t*-test was applied for comparison between control and ZnO NP or $ZnSO_4$ groups. Differences were considered as statistically significant at values of $^{*}p < 0.05$ and $^{**}p < 0.01$.

CRediT authorship contribution statement

Zhiling Guo: Conceptualization, Methodology, Validation, Investigation, Formal analysis, Writing - original draft, Writing - review & editing, Visualization. **Peng Zhang:** Conceptualization, Methodology, Validation, Investigation, Writing - original draft, Writing - review & editing, Visualization. **Yali Luo:** Investigation. **Heidi Qunhui Xie:** Writing - review & editing. **Swaroop Chakraborty:** Investigation. **Fazel Abdolahpur Monikh:** Writing - review & editing. **Lijing Bu:** Formal analysis. **Yiyun Liu:** Investigation. **Yongchao Ma:** Investigation. **Zhiyong Zhang:** Resources. **Eugenia Valsami-Jones:** Writing - review & editing. **Bin Zhao:** Supervision, Resources, Funding acquisition. **Iseult Lynch:** Conceptualization, Writing - review & editing.

Declaration of Competing Interest

The authors declare no competing financial interest.

Acknowledgments

This work was supported by the National Natural Science Foundation of China (Grant Nos. 21836004, 91543204, and 21525730), the Strategic Priority Research Program of the Chinese Academy of Sciences (Grant No. XDB14030400), the National Key Research and Development Program of China (Grant No. 2018YFA0901103). Marie Skłodowska-Curie Individual Fellowships (NanoBBB Grant Agreement No. 798505 to Z. Guo; NanoLabels Grant Agreement No. 750455 to P. Zhang) under the European Union's Horizon 2020 research program were acknowledged. Technical support from the Shanghai Applied Protein Technology facility (Shanghai, China) is gratefully acknowledged.

Appendix A. Supplementary data

Supplementary material related to this article can be found, in the online version, at doi:https://doi.org/10.1016/j.nantod.2020.100977.

References

[1] M.R. Gwinn, V. Vallyathan, Environ. Health Perspect. 114 (2006) 1818–1825.
[2] F. Piccinno, F. Gottschalk, S. Seeger, B. Nowack, J. Nanopart. Res. 14 (2012) 1109.
[3] M.J. Osmond, M.J. Mccall, Nanotoxicology 4 (2010) 15–41.
[4] A. Becheri, M. Dürr, P.L. Nostro, P. Baglioni, J. Nanopart. Res. 10 (2008) 679–689.
[5] K.S. Siddiqi, A. ur Rahman, A. Husen, Nanoscale Res. Lett. 13 (2018) 141.
[6] H. Mirzaei, M. Darroudi, Ceramics Int. 43 (2017) 907–914.
[7] H. Zhang, B. Chen, H. Jiang, C. Wang, H. Wang, X. Wang, Biomaterials 32 (2011) 1906–1914.
[8] R. Andrzejak, J. Antonowicz, Z. Andreasik, Med. Pr. 43 (1992) 329–333.
[9] W.G. Kreyling, Toxicol. Appl. Pharm. 299 (2016) 41–46.
[10] Y.-Y. Kao, T.-J. Cheng, D.-M. Yang, C.-T. Wang, Y.-M. Chiung, P.-S. Liu, J. Mol. Neurosci. 48 (2012) 464–471.
[11] C. Aijie, L. Huimin, L. Jia, O. Lingling, W. Limin, W. Junrong, L. Xuan, H. Xue, S. Longquan, Nanomedicine 12 (2017) 2453–2470.
[12] W.-S. Cho, B.-C. Kang, J.K. Lee, J. Jeong, J.-H. Che, S.H. Seok, Part. Fibre Toxicol. 10 (2013) 9.
[13] A. Karmakar, Q. Zhang, Y. Zhang, J. Food Drug Anal. 22 (2014) 147–160.
[14] S. Sudhakaran, S. Athira, P. Mohanan, Neurotoxicology 73 (2019) 213–227.
[15] A. Nicolosi, L. Cardoit, P. Pasquereau, C. Jaillet, M. Thoby-Brisson, L. Juvin, D. Morin, Neurotoxicology 67 (2018) 150–160.
[16] A. Yaqub, I. Faheem, K.M. Anjum, S.A. Ditta, M.Z. Yousaf, F. Tanvir, C. Raza, Appl. Nanosci. (2019) 1–9.
[17] H. Liu, H. Yang, Y. Fang, K. Li, L. Tian, X. Liu, W. Zhang, Y. Tan, W. Lai, L. Bian,Sci. Total Environ. (2019), 135809.
[18] B. Wang, Q. Wang, H. Chen, X. Zhou, H. Wang, H. Wang, J. Zhang, W. Feng, J. Nanosci. Nanotechnol. 16 (2016) 5553–5561.
[19] J. Wang, Y. Liu, F. Jiao, F. Lao, W. Li, Y. Gu, Y. Li, C. Ge, G. Zhou, B. Li, Toxicology 254 (2008) 82–90.
[20] P. Zhang, S. Misra, Z. Guo, M. Rehkämper, E. Valsami-Jones, Nat. Protoc. 14 (2019) 2878–2899.
[21] J. Szelényi, Brain Res. Bull. 54 (2001) 329–338.
[22] Z. Guo, Y. Luo, P. Zhang, A.J. Chetwynd, H.Q. Xie, F.A. Monikh, W. Tao, C. Xie, Y. Liu, L. Xu,Environ. Int. 136 (2020), 105437.
[23] Z. Guo, Q. Hu, J. Tian, L. Yan, C. Jing, H.Q. Xie, W. Bao, R.H. Rice, B. Zhao, G. Jiang, Environ. Pollut. 218 (2016) 34–38.
[24] B.D. Drever, G. Riedel, B. Platt, Behav. Brain Res. 221 (2011) 505–514.
[25] Z. Gu, P.W. Lamb, J.L. Yakel, J. Neurosci. 32 (2012) 12337–12348.
[26] J. Cedernaes, M. Schönke, J.O. Westholm, J. Mi, A. Chibalin, S. Voisin, M. Osler, H. Vogel, K. Hörnaeus, S.L. Dickson,Sci. Adv. 4 (2018), eaar8590.
[27] M.L. Fournier, A. Paulson, N. Pavelka, A.L. Mosley, K. Gaudenz, W.D. Bradford, E. Glynn, H. Li, M.E. Sardiu, B. Fleharty, Mol. Cell. Proteomics 9 (2010) 271–284.
[28] P. Nagy, I. Aubert, Neuroscience 218 (2012) 1–11.
[29] P. Fagone, S. Jackowski, BBA-Mol. Cell Biol. L. 1831 (2013) 523–532.
[30] J.R. Atack, C. May, J.A. Kaye, A.D. Kay, S.I. Rapoport, Ann. Neurol. 23 (1988) 161–167.
[31] T. Davis, Lancet 2 (1976) 1403.
[32] M.-S. García-Ayllón, I. Riba-Llena, C. Serra-Basante, J. Alom, R. Boopathy, J. Sáez-Valero, PLoS One 5 (2010) e8701.
[33] D. Dingova, T. Fazekas, P. Okuliarova, J. Strbova, M. Kucera, A. Hrabovska, J. Alzheimers Dis. 51 (2016) 801–813.
[34] J.P. Dzoyem, V. Kuete, J.N. Eloff, Biochemical parameters in toxicological studies in Africa: significance, principle of methods, data interpretation, and use in plant screenings, in: Toxicological Survey of African Medicinal Plants, Elsevier, 2014, pp. 659–715.
[35] F.M. Farahat, C.A. Ellison, M.R. Bonner, B.P. McGarrigle, A.L. Crane, R.A. Fenske, M.R. Lasarev, D.S. Rohlman, W.K. Anger, P.J. Lein, Environ. Health Perspect. 119 (2011) 801–806.
[36] H.Q. Xie, H.-M. Xu, H.-L. Fu, Q. Hu, W.-J. Tian, X.-H. Pei, B. Zhao, Environ. Health Perspect. 121 (2013) 613–618.
[37] T.M. Sager, D.W. Porter, V.A. Robinson, W.G. Lindsley, D.E. Schwegler-Berry, V. Castranova, Nanotoxicology 1 (2007) 118–129.
[38] W.-S. Cho, R. Duffin, S.E. Howie, C.J. Scotton, W.A. Wallace, W. MacNee, M. Bradley, I.L. Megson, K. Donaldson, Part. Fibre Toxicol. 8 (2011) 1.

[39] M. Zimmermann, Br. J. Pharmacol. 170 (2013) 953–967.
[40] S.D. Gower-Winter, C.W. Levenson, Biofactors 38 (2012) 186–193.
[41] A. Takeda, Brain Res. Rev. 34 (2000) 137–148.
[42] A. Prakash, K. Bharti, A.B.A. Majeed, Fund. Clin. Pharmacol. 29 (2015) 131–149.
[43] S.M. Hancock, D.I. Finkelstein, P.A. Adlard, Front. Aging Neurosci. 6 (2014) 137.
[44] A.I. Bush, W.H. Pettingell, G. Multhaup, M. d Paradis, J.-P. Vonsattel, J.F. Gusella, K. Beyreuther, C.L. Masters, R.E. Tanzi, Science 265 (1994) 1464–1467.
[45] J.C. King, D.M. Shames, L.R. Woodhouse, J. Nutr. 130 (2000) 1360S–1366S.
[46] S.E. Nasrabady, B. Rizvi, J.E. Goldman, A.M. Brickman, Acta Neuropathol. Comm. 6 (2018) 22.
[47] R. Wang, P.H. Reddy, J. Alzheimers Dis. 57 (2017) 1041–1048.
[48] I. Grissa, S. Guezguez, L. Ezzi, S. Chakroun, A. Sallem, E. Kerkeni, J. Elghoul, L. El Mir, M. Mehdi, H. ben Cheikh, Environ. Sci. Pollut. Res. 23 (2016) 20205–20213.
[49] G.L. Ellman, K.D. Courtney, V. Andres Jr, R.M. Featherstone, Biochem. Pharmacol. 7 (1961) 88–95.
[50] L. Whitmore, B. Wallace, Nucleic Acids Res. 32 (2004) W668–W673.

Zhiling Guo obtained her PhD (2014) at the University of Chinese Academy of Sciences (CAS), with part of the project completed at University of Connecticut (USA). Then she worked as a postdoctoral fellow at Research Center for Eco-Environmental Sciences (CAS) for two years, where she studied the molecular toxicity of dioxin, arsenic and nanomaterials. After that she worked at McGill University (Canada) as a postdoctoral fellow, focusing on neuropsychopharmacology. She is currently working at the School of Geography, Earth and Environmental Sciences, University of Birmingham, UK. Her research interests include molecular toxicity and neurotoxicity of contaminants including engineered nanomaterials.

Peng Zhang obtained PhD (2013) in Bioinorganic Chemistry from University of Chinese Academy of Sciences. He was an associate professor in Institute of High Energy Physics (CAS) from 2015 to 2018. He is currently working at the School of Geography, Earth and Environmental Sciences, University of Birmingham, UK. His research interests are in the area of nanosafety, toxicology, nanomaterial application in agriculture and environmental remediation.

Zhiyong Zhang holds a PhD in radiochemistry from Peking University. He is now a Professor and scientific leader in environmental health and safety at the CAS Key Lab for Biomedical Effects of Nanomaterials and Nanosafety, Institute of High Energy Physics, CAS. His current research interests are coordination chemistry, bioinorganic chemistry, and environmental chemistry of rare earth elements, as well as the toxicology and ecotoxicology of nanomaterials.

Eugenia (Éva) Valsami-Jones is a Professor of Environmental Nanoscience at the University of Birmingham, where she is also Director of the Facility for Environmental Nanoscience Analysis and Characterisation and Director of the MRes on Environmental and Biological Nanoscience. She coordinates H2020 project ACEnano and leads the European Commission's NanoSafety Cluster. Her research focuses on nanoscale processes in a biological and environmental context. She has pioneered traceable stable-isotope labelled nanomaterials and developed analytical solutions for complex nanoscale characterisation. She was the Mineralogical Society's Distinguished Lecturer for 2015 and the Distinguished Guest Lecturer and Medalist of the Royal Society of Chemistry for 2015. She is currently a Royal Society Wolfson Fellow.

Bin Zhao obtained his PhD (2002) in Biology from Hong Kong University of Science and Technology. He is a Professor in State Key Laboratory of Environmental Chemistry and Ecotoxicology, Research Center for Eco-Environmental Sciences, CAS. His current research interests are focusing on health effects and molecular mechanisms of action of environmental contaminants, development and application of high-throughput bioanalytical methods for analysis of emerging pollutants.

Iseult Lynch holds a PhD in Chemistry from University College Dublin, Ireland. She is Chair (Professor) of Environmental Nanosciences at the School of Geography, Earth and Environmental Sciences, University of Birmingham (UoB). She was recently awarded the 2020 John Jeyes prize for Environmental Sciences from the Royal Society of Chemistry for her research into the impacts of the acquired ecological corona on nanomaterials ecotoxicity. Her research interests span human and environmental impacts of engineered and anthropogenic nanoscale materials including development of predictive models and environmental applications of nanomaterials.